Charge Neutral Current Generation in a Spontaneous Quantum Hall Antiferromagnet

Miuko Tanaka, Yuya Shimazaki, Ivan Valerievich Borzenets, Kenji Watanabe, Takashi Taniguchi, Seigo Tarucha, and Michihisa Yamamoto

Phys. Rev. Lett. **126**, 016801 — Published 6 January 2021

DOI: 10.1103/PhysRevLett.126.016801

Charge neutral current generation in a spontaneous quantum Hall antiferromagnet

Miuko Tanaka[1], Yuya Shimazaki[2], Ivan Valerievich Borzenets[3], Kenji Watanabe[4], Takashi Taniguchi[4], Seigo Tarucha[5], and Michihisa Yamamoto[5]

[1]Department of Applied Physics, University of Tokyo, Bunkyo-ku, Japan. [2]Institute of Quantum Electronics, ETH Zurich, Zurich, Switzerland. [3]Department of Physics, City University of Hong Kong, Hong Kong. [4]National Institute for Materials Science, Tsukuba-shi, Japan. [5]Center for Emergent Matter Science, RIKEN, Wako-shi, Japan

Intrinsic Hall effect allows for generation of a non-dissipative charge neutral current, such as a pure spin current generated via the spin Hall effect. Breaking of the spatial inversion or time reversal symmetries, or the spin-orbit interaction is generally considered necessary for generation of such a charge neutral current. Here we challenge this general concept and present generation and detection of a charge neutral current in a centrosymmetric material with little spin-orbit interaction. We employ bilayer graphene, and find enhanced nonlocal transport in the quantum Hall antiferromagnetic state, where spontaneous symmetry breaking occurs due to the electronic correlation.

A charge neutral current such as a pure spin current is promising for future low-energy consumption devices because it does not accompany Joule heating [1,2]. While Hall effect allows for mutual conversion between a charge neutral current and an electric field [3], the role of the electronic correlation effect in this phenomenon has not yet been well understood.

Electron correlated systems are generally sensitive to external perturbations and undergo various phase transitions under the change of control parameters. The correlation effect becomes important when the interaction energy is dominant over the kinetic energy, such as in the case of a flat band. An electron correlated system is achieved in a two-dimensional electron system by application of a perpendicular magnetic field, when the kinetic energy is quenched in Landau levels. For the existence of additional degree of freedoms (DOF) of electrons, such as the spin, layer, and valley, the electronic interaction leads to splitting of Landau levels to gain the exchange energy [4,5]. Such splitting of Landau levels and emergence of an ordered phase takes place in the quantum Hall states of monolayer and bilayer graphene.

Due to their zero-gap feature, monolayer and bilayer graphene have a Landau level at zero energy, called as zero-th Landau level. Emergence of a gapped $\nu=0$ state (ν is the filling factor) due to the splitting of zero-th Landau level has been experimentally observed both in monolayer and bilayer graphene [6-22]. There has been a long theoretical debate on the nature of $\nu=0$ state [23-36]. According to the recent coincidence between a theory [23] and a transport experiment under a tilted magnetic field [14], the most-likely state of bilayer graphene at low temperature is a canted layer antiferromagnet (CAF), where spins tend to align ferromagnetically due to the exchange interaction within each layer but anti-ferromagnetically between the layers (Fig.1a). The CAF state has two unique features, which are distinct from those of conventional quantum Hall magnets in semiconductor-based two-dimensional electron systems. First, non-zero spin and valley contrasting Hall conductivity is theoretically expected [36, 23], although it is experimentally elusive. Second, absence of edge channels was reported experimentally [10-18], and theoretically explained by valley scattering at sample edges [23,24], in spite of the expected Hall conductivity.

Owing to these two unique properties, the CAF state in bilayer graphene is a suitable system to study a new way of charge neutral current generation. When a charge current is injected, a “spin-valley current”, which we define as the difference of valley current between the spins, flows perpendicularly to the injected current (Fig. 1b) owing to the spin and valley contrasting Hall conductivity. Because there is no edge channel, a non-dissipative spin-valley current flows through the bulk region. We call this phenomenon the “spin-valley Hall effect”. Existence of the spin-valley current seems to have been overlooked because it carries neither spin nor valley degree of freedom.

The spin-valley Hall effect is phenomenologically similar to the spin Hall effect [3] and valley Hall effect [37, 38, 44-46], both of which have been extensively studied. However, the spin-valley current is very different from other charge neutral currents reported in previous researches in terms of symmetry and electron correlation. Generally, to realize non-zero Hall conductivity for each spin or valley, either the spin-orbit interaction or the breaking of spatial inversion or time reversal symmetries is necessary. In previous experimental studies, enhanced spin-orbit interaction by adatom doping or substrates effect were used in materials with weak spin-orbit interaction [39-43], and symmetries were broken by one-body effects such as non-centrosymmetric crystal structures [44-46] and application of an external electric field [37, 38]. In the CAF state, the spatial inversion and time reversal symmetries are broken spontaneously due to the electronic interaction [36, 23]. Because this interaction effect is sensitive to the filling factor and out-of-plane electric field, charge neutral current generation in the CAF state is gate tunable.

Another important distinction of the spin-valley Hall effect in terms of application is that it allows for coupling of the spin and valley DOFs. Because the Hall conductivity is spin and valley contrasting, if we inject an opposite current for each spin, or a spin current, a valley current is expected to flow in the transverse direction (Fig. 1c). While the spin-orbit interaction is weak in graphene, this mutual conversion between the spin current and valley current may open up a new possibility of electrical generation and detection of a spin current in graphene with high efficiency.

We fabricate Hall bars of bilayer graphene encapsulated in hexagonal boron nitride (h-BN) (Fig. 1d, e) by mechanical exfoliation, dry transfer, and side contact methods [47]. By applying voltages to the graphite (Hall bar 1) or p-doped Si (Hall bar 2) back gate and gold top gate, the carrier density n and out-of-plane electric field (displacement field) D are tuned independently.

We study generation and detection of the charge neutral spin-valley current in the CAF state of bilayer graphene using nonlocal transport measurement. Nonlocal transport measurement is a well-established technique to study the spin Hall effect and valley Hall effect [3, 37, 38, 46, 50]. When a charge current is injected between the terminals 2 and 6 of Fig. 1e, a charge neutral current is generated. Because of the non-dissipative nature of the charge neutral current, it can flow in the longitudinal direction of the Hall bar over distances of few microns. Voltage is then induced between the terminals 3 and 5, owing to the inverse Hall effect. The nonlocal resistance R_{NL} is defined as the ratio of the injected current to the detected nonlocal voltage V_{3-5}/I_{2-6}.

Previously, a large nonlocal resistance under an application of perpendicular magnetic field was reported for monolayer graphene [50]. It was interpreted as “Zeeman spin Hall effect”, where a spin current is generated due to Zeeman splitting at the charge neutral point (CNP). While the spin splitting ground state has been denied by recent understanding of the CAF state, their scenario is common with our proposal of the spin-valley Hall effect in a sense that the nonlocal resistance originates from a charge neutral current. However, previous study [50] had no experimental evidence of the charge neutral current generation as an origin of the nonlocal resistance. In our study, we observe characteristic scaling behavior of the nonlocal transport varying the magnetic field and temperature, which evidences the charge neutral current generation. In addition, based on recent understanding of the phase diagram of $\nu=0$ state, we identify the spin-valley Hall effect by significant enhancement of the nonlocal resistance at the CAF state in dual-gated bilayer graphene.

In addition, to eliminate the possibility of edge transport as another origin of the large nonlocal resistance, we employ two Hall bars (Hall bars 1 and 2) with the same dimension of the active area but with different edge length by adding extra protruding part between the terminals 2 and 3 in one of the Hall bars (Hall bar 1) (Fig. 1d). We confirm that the value of nonlocal resistance is comparable, implying that the edge transport is not the origin of the enhanced nonlocal resistance and that the charge neutral current flows in the bulk, as we see in the following.

We first measured the local resistance $R_L = V_{2-3}/I_{1-4}$ at temperature T=1.7 K in the linear transport regime (I_{1-4} < 5 nA) to identify the CAF state. Figs. 2a-c are dual gate dependence of R_L obtained with Hall bar 2 (Fig. 1d) shown as a function of carrier density n and displacement field D obtained for various perpendicular magnetic fields. At zero magnetic field, R_L at the CNP monotonically increases with the displacement field D due to the opening of the single particle band gap. When the magnetic field of 2 T is applied, a local maximum appears around the D=0 and n=0 indicating development of the CAF insulating state (Fig. 2d) [14, 19, 22]. This state becomes more robust with increasing magnetic field due to the reduced kinetic energy. When the displacement field is increased from zero, R_L at the CNP once decreases and again increases. This upturn is attributed to closing of the CAF gap and phase transition to another insulating state, layer polarized (LP) state as reported in previous studies [14, 19, 22].

We then performed nonlocal transport measurement for the CAF state. Figs. 2e and 2f show the n and D dependence of R_{NL} under the magnetic field of 2 T and 4 T, respectively. Similarly to R_L, R_{NL} becomes maximal at $D = 0$ and $n = 0$. The peak value of R_{NL} is 10^4 times larger than that expected for the trivial classical current diffusion obtained from R_L and van der Pauw formula [51]. R_{NL} is suppressed at the phase boundary between the CAF and LP states, and has the same order of magnitudes in these two insulating states (Fig. 2e, Fig. S9). This indicates the same order of generation efficiency and decay of the charge neutral current, which is reasonable because both charge neutral currents are expected to be scattered only by atomically sharp defects or at sample edges [37, 38].

Figs. 2g and 2h show the carrier density dependence of R_L and R_{NL} at $D = 0$ under the magnetic field of 0 to 8 T. The peak of R_{NL} is sharper than that of R_L implying a nonlinear relationship between R_L and R_{NL} as discussed in the following [57]. Similar results were also obtained for the Hall bar 1 [58].

We now turn to the relationship between R_L and R_{NL}. We measure R_L and R_{NL} for D=0 while sweeping the temperature from 1.7 to 32 K with the magnetic field as a parameter. The temperature in this range is less than the energy gap of the CAF state estimated from the boundary displacement field between the CAF state and the LP state, which is proportional to the magnetic field: $\Delta_{\mathrm{CAF}}/B \sim 40\,\mathrm{K/T}$ [21, 59]. We then plot the peak values of R_{NL} vs R_L (at n~0, see Figs. 2g and 2h) in Fig. 3. We find that all data points obtained with Hall bar 1 fall on a single curve of the cubic scaling for 20 kΩ< R_L < 80 kΩ. In Hall bar 2, we observe linear scaling for R_L exceeding 90 kΩ. Below R_L~90 kΩ, the scaling exponent becomes larger and becomes cubic below R_L~30 kΩ.

Similarly to the spin Hall effect and valley Hall effect [3, 37, 38, 46], R_{NL} arising from the spin-valley Hall effect and inverse spin-valley Hall effect is given by the established formula,

$$R_{\mathrm{NL}} = \frac{W}{2l}\frac{{\sigma_H}^2}{\sigma_{xx}({\sigma_{xx}}^2+{\sigma_H}^2)}\mathrm{e}^{-L/l} \quad (1)$$

for a homogeneous semiclassical system. Here σ_{xx} is the local electrical conductivity, σ_H is the spin-valley Hall conductivity defined as the driven spin-valley current density divided by the transverse in-plane electric field, W is the Hall bar width, L is the Hall bar length, and l is the scattering length of the spin-valley current. Assuming the intrinsic mechanism of the Hall conductivity, σ_H is constant. R_L and R_{NL} should then have the cubic scaling relationship $R_{\mathrm{NL}} \propto \rho^3$ for $\sigma_{xx} \gg \sigma_H$ and linear scaling relationship $R_{\mathrm{NL}} \propto \rho$ for $\sigma_{xx} \ll \sigma_H$. This intrinsic scenario can account for our experimental result. Obtained scaling relationship is the evidence of nonlocal transport mediated by a charge neutral current generated by the intrinsic Hall effect. The absolute value of R_{NL} is also in a reasonable range for the theoretical value of $\sigma_H = 4e^2/h$ in Eq. 1 and comparable with the value obtained in previous studies on the nonlocal transport of valley Hall effect in bilayer graphene [37, 38, 60].

Equation (1) indicates that scaling crossover from cubic to linear occurs around $\rho =$

$h/4e^2 \sim 6.45\ \mathrm{k\Omega}$. However, Hall bar 1 exhibits cubic scaling in all data up to $\rho \sim 23\ \mathrm{k\Omega}$ and Hall bar 2 exhibits cubic scaling up to $\rho \sim 17\ \mathrm{k\Omega}$. Unexpected cubic scaling for the large ρ was also observed in previous experiments on the valley Hall effect in bilayer graphene [38, 60]. Although the reason for this contradiction is not yet understood, one possibility is that the charge conductivity σ_{xx} in Eq. (1) may not simply be measured by the electrical current divided by the in-plane electric field, but be defined as effective conductivity for the thermally activated carriers [37]. Another possibility is that the spin-valley Hall conductivity is reduced due to sample dependent inhomogeneity.

To summarize our experimental findings, we observe significant enhancement of the nonlocal resistance at the CAF state, and cubic and linear scaling relationship between the local and nonlocal resistance. The observed scaling is consistent with the theoretical expectation of the spin-valley Hall effect and implies that the origin of the enhanced nonlocal resistance is the generation of a charge neutral current by the intrinsic Hall effect.

To further make sure this scenario, we here discuss four other possible contributions to the nonlocal resistance to show that their contribution is minor.

First, current leakage through voltage measurement terminals makes additional contribution to the nonlocal resistance when the input impedance of voltage amplifiers is not high enough [37,38]. However, this contribution is confirmed to be small enough by estimation and control measurement in different voltage amplifiers [51].

Second, AC measurement can cause artifact of nonlocal resistance due to the finite capacitance between measurement lines and ground. However, this contribution is negligible since the measured nonlocal resistances in lock-in measurement are identical for two different reference frequencies [51].

Third, thermal flow can also cause nonlocal resistance due to the Ettingshausen and Nernst effect [61]. The value of nonlocal resistance due to the thermal effect estimated based on previous researches on thermal properties of graphene is too small to account for the measured large R_{NL} at least above B=4 T [51], where we observe cubic and linear scaling between R_L and R_{NL}. In a lower magnetic field of less than 2 T, the thermal effect may become dominant. This might be responsible for the deviation of the scaling relationship from the expected one for the low magnetic field in Fig. 3.

Finally, another possible origin of nonlocal resistance is current flow along the sample edge. Although established both experimentally [10-18] and theoretically [23,24] that the CAF state does not have an edge channel, gate inhomogeneity at the sample edge can cause carrier doping and produce less-resistive regions along the edge. As already mentioned, we have prepared Hall bars with different edge lengths but with the same dimension of the active area (Fig. 1d). Hall bar 1 has a 10 times longer edge between the terminals 2 and 3 compared to that of Hall bar 2. Suppose carrier transport occurs only at the edges, R_{NL} defined as the ratio of the injected current to the detected nonlocal voltage (V_{3-5}/I_{2-6} in Fig. 1d, e) should be 10 times smaller for the long-edge Hall bar (Hall bar 1). As shown in Fig. 3, however, the values of nonlocal resistance are comparable for the two Hall bars. This result cannot be assigned to the edge contribution but is consistent with the charge neutral current in the bulk as the main contribution. In addition, we measured comparable values of nonlocal resistance for two other Hall bars with different edge lengths (Fig. S4).

Thus all other possible contributions to the nonlocal resistance are minor and the majority of the signal is assigned to the generation of a bulk charge neutral current by the intrinsic Hall conductivity in the CAF state.

In this work, we have not directly identified the Hall effect for each spin and valley. Demonstration of the conversion between the valley current and spin current at the CAF state should directly evidence that the intrinsic Hall conductivity is spin and valley contrasting.

Since the valley Hall angle defined as the induced valley current divided by the driving electrical current in the valley Hall effect is higher than the spin Hall angle of most of the materials currently available in spintronics, the spin-valley Hall effect may allow for generation of a spin current at high efficiency when combined with the valley Hall effect. We also note that application of a perpendicular magnetic field may not be necessary in future. Using a flatter band available for example in ABC-stacked several layers graphene, the CAF (or AF) gap can exceed room temperature at zero external magnetic field [6-9, 11, 13]. Our work thus demonstrated a promising principle to generate a charge neutral current in electron correlated states.

M. Y. and S. T. acknowledge support from KAKENHI (Grant No. 26220710, 17H01138). I.V.B. acknowledges CityU New Research Initiatives/Infrastructure Support from Central (APRC): 9610395, and the Hong Kong Research Grants Council (ECS) Project: 9048125. K.W. and T.T. acknowledge the Elemental Strategy Initiative conducted by the MEXT, Japan and the CREST (JPMJCR15F3), JST.

References

[1] I. Zutic, J. Fabian, and S. D. Sarma, "Spintronics: Fundamentals and applications", Rev. Mod. Phys. 76, 323 (2004).

[2] S. A. Wolf, D. D. Awschalom, R. A. Buhrman, J. M. Daughton, S. von Molnar, M. L. Roukes, A. Y. Chtchelkanova, and D. M. Treger, "Spintronics: A Spin-Based Electronics Vision for the Future", Science 294, 1488 (2001).

[3] J. Sinova, S. O. Valenzuela, J. Wunderlich, C. H. Back, T. Jungwirth, "Spin Hall effect", Rev. Mod. Phys. 87, 1213 (2015).

[4] S. M. Girvin and A. H. MacDonald in "Perspectives in Quantum Hall Effects", S. Das Sarma and A. Pinczuk, eds. (John Wiley & Sons, 1997).

[5] Girvin, S. M. The Quantum Hall Effect: Novel Excita- tions and Broken Symmetries. In Comtet, A., Jolicœur, T., Ouvry, S. & David, F. (eds.) Les Houches Lecture Notes, in: Topological Aspects of Low Dimensional Sys- tems, vol 69, 53-175 (Springer-Verlag, 2000).

[6] J. Velasco Jr, L. Jing, W. Bao, Y. Lee, P. Kratz, V. Aji, M. Bockrath, C. N. Lau, C. Varma, R. Stillwell, D. Smirnov, Fan Zhang, J. Jung and A. H. MacDonald, "Transport spectroscopy of symmetry-broken insulating states in bilayer graphene ", Nature Nanotechnol. **7**, 156 (2012).

[7] F. Freitag, J. Trbovic, M. Weiss, and C. Schönenberger, "Spontaneously gapped ground state in suspended bilayer graphene", Phys. Rev. Lett. **108**, 076602 (2012).

[8] Y. Lee, D. Tran, K. Myhro, J. Velasco, N.Gillgren, C. N. Lau, Y. Barlas, J. M. Poumirol, D. Smirnov, and F. Guinea, "Competition between spontaneous symmetry breaking and single-particle gaps in trilayer graphene ", Nature Comm. **5**, 5656 (2014).

[9] W. Bao, J. Velasco Jr., F. Zhang, L. Jing, B. Standley, D. Smirnov, M. Bockrath, A. H. MacDonald, C. N. Lau, "Evidence for a spontaneous gapped state in ultraclean bilayer graphene", PNAS 109, 10802 (2012).

[10] Y. Zhao, P. Cadden-Zimansky, Z. Jiang, and P. Kim, "Symmetry breaking in the zero-energy Landau level in bilayer graphene ", Phys. Rev. Lett. **104**, 066801 (2010).

[11] R. T. Weitz, M. T. Allan, B. E. Feldman, J. Martin, A. Yacoby, "Broken-symmetry states in doubly gated suspended bilayer graphene", Science **330**, 812 (2010).

[12] S. Kim, K. Lee, and E. Tutuc, "Spin-polarized to valley-polarized transition in graphene bilayers at $\nu = 0$ in high magnetic fields", Phys. Rev. Lett. **107**, 016803 (2011).

[13] A. Veligura, H. J. van Elferen, N. Tombros, J. C. Maan, U. Zeitler, and B. J. van Wees, "Transport gap in suspended bilayer graphene at zero magnetic field", Phys. Rev. B **85**, 155412 (2012).

[14] P. Maher, C. R. Dean, A. F. Young, T. Taniguchi, K. Watanabe, K. L. Shepard, J. Hone, and P. Kim, "Evidence for a spin phase transition at charge neutrality in bilayer graphene", Nature Phys. **9**, 154 (2013).

[15] J. G. Checkelsky, L. Li, and N. P. Ong, "Zero-Energy State in Graphene in a High Magnetic Field", Phys. Rev. Lett. **100**, 206801 (2008).

[16] A. J. M. Giesbers, L. A. Ponomarenko, K. S. Novoselov, A. K. Geim, M. I. Katsnelson, J. C. Maan, and U. Zeitler, "Gap opening in the zeroth Landau level of graphene", Phys. Rev. Lett. **98**, 196806 (2007).

[17] D. A. Abanin, K. S. Novoselov, U. Zeitler, P. A. Lee, A. K. Geim, and L. S. Levitov, "Dissipative Quantum Hall Effect in Graphene near the Dirac Point", Phys. Rev. Lett. **98**, 196806 (2007).

[18] B. E. Feldman, J. Martin, and A. Yacoby, "Broken-symmetry states and divergent resistance in suspended bilayer graphene", Nature Phys. **5**, 889 (2009).

[19] K. Lee, B. Fallahazad, J. Xue, D. C. Dillen, K. Kim, T. Taniguchi, K. Watanabe, E. Tutuc, "Chemical potential and quantum Hall ferromagnetism in bilayer graphene", Science **345**, 58 (2014).

[20] S. Pezzini, C. Cobaleda, B. A. Piot, V. Bellani, and E. Diez, "critical point for the canted antiferromagnetic to ferromagnetic phase transition at charge neutrality in bilayer graphene", Phys. Rev. B **90**, 121404(R) (2014).
[21] J. Li, Y. Tupikov, K. Watanabe, T. Taniguchi, and J. Zhu, "Effective Landau Level Diagram of Bilayer Graphene", Phys. Rev. Lett. **120**, 047701 (2018).
[22] J. Li, H. Fu, Z. Yin, K. Watanabe, T. Taniguchi, J. Zhu, "Metallic phase and temperature dependence of the ν=0 quantum Hall state in bilayer graphene", Phys. Rev. Lett. 122, 097701 (2019).
[23] M. Kharitonov, "Canted Antiferromagnetic Phase of the $\nu = 0$ Quantum Hall State in Bilayer Graphene", Phys. Rev. Lett. **109**, 046803 (2012).
[24] J. Jung and A. H. MacDonald, "Theory of the magnetic-field-induced insulator in neutral graphene sheets", Phys. Rev. B **80**, 235417 (2009).
[25] J. Lambert and R. Côté, "Quantum Hall ferromagnetic phases in the Landau level N = 0 of a graphene bilayer", Phys. Rev. B **87**, 115415 (2013).
[26] K. Nomura, and A. H. MacDonald, "Quantum Hall Ferromagnetism in Graphene", Phys. Rev. Lett. **96,** 256602 (2006).
[27] J. Alicea, and M. P. A. Fisher, "Graphene integer quantum Hall effect in the ferromagnetic and paramagnetic regimes", Phys. Rev. B **74,** 075422 (2006).
[28] M. O. Goerbig, R. Moessner, and B. Douçot, "Electron interactions in graphene in a strong magnetic field", Phys. Rev. B **74,** 161407 (2006).

[29] E. V. Gorbar, "Broken symmetry $\nu = 0$ quantum Hall states in bilayer graphene: Landau level mixing and dynamical screening" Phys. Rev. B **85,** 235460 (2012).
[30] E. V. Castro, N. M. R. Peres, T. Stauber, and N. A. P. Silva, "Low-Density Ferromagnetism in Biased Bilayer Graphene", Phys. Rev. Lett. **100**, 186803 (2008).
[31] R. Nandkishore and L. Levitov, "Quantum anomalous Hall state in bilayer graphene", Phys. Rev. B **82**, 115124 (2010).
[32] O. Vafek and K. Yang, "Many-body instability of Coulomb interacting bilayer graphene: Renormalization group approach", Phys. Rev. B **81**, 041401 (2010).
[33] Y. Lemonik, I. L. Aleiner, C. Toke, and V. I. Fal'ko, "Spontaneous symmetry breaking and Lifshitz transition in bilayer graphene", Phys. Rev. B **82**, 201408 (2010).
[34] M. Kharitonov, "Antiferromagnetic state in bilayer graphene", Phys. Rev. B **86**, 195435 (2012).
[35] G. Murthy, E. Shimshoni, and H. A. Fertig, "Spin-valley coherent phases of the $\nu = 0$ quantum Hall state in bilayer graphene", Phys. Rev. B **96**, 245125 (2017).
[36] F. Zhang, J. Jung, G. A. Fiete, Q. Niu, and A. H. MacDonald, "Quantum Hall States in Chirally Stacked Few-Layer Graphene Systems″, Phys. Rev. Lett. **106**, 156801 (2011).
[37] Y. Shimazaki, M. Yamamoto, I. V. Borzenets, K. Watanabe, T. Taniguchi & S. Tarucha, "Generation and detection of pure valley current by electrically induced Berry curvature in bilayer graphene", Nature Phys. **11,** 1032 (2015).
[38] M. Sui, G. Chen, L. Ma, W. Shan, D. Tian, K. Watanabe, T. Taniguchi, X. Jin, W. Yao, D. Xiao, Y. Zhang, "Gate-tunable topological valley transport in bilayer graphene", Nature Phys. **11,** 1027 (2015).
[39] J. Balakrishnan, G. K. W. Koon, M. Jaiswal, A. H. C. Neto, B. Ozyilmaz, "Colossal enhancement of spin-orbit coupling in weakly hydrogenated graphene." Nat. Phys. **9**, 284 (2013).
[40] J. Balakrishnan, G. K. W. Koon, A. Avsar, Y. Ho, J. H. Lee, M. Jaiswal, S. J. Baeck, J. H. Ahn, A. Ferreira, M. A. Cazalilla, A. H. C. Neto, B. Ozyilmaz, "Giant spin Hall effect in graphene grown by chemical vapour deposition." Nat. Commun. **5**, 4748 (2014).
[41] A. Avsar, J. Tan, T. Taychatanapat, J. Balakrishnan, G. K. W. Koon, Y. Yeo, J. Lahiri, A. Carvalho, A. S. Rodin, E. C. T. O'Farrell, G. Eda, A. H. C. Neto, B. Ozyilmaz, "Spin-orbit proximity effect in graphene.", Nat. Commun. **5**, 4875 (2015).
[42] C. K. Safeer, J. I-Aynes, F. Herling, J. H. Garcia, M. Vila, N. Ontoso, M. R. Calvo, S. Roche, L. E. Hueso, F. Casanova, "Room-temperature Spin Hall Effect in Graphene/MoS2 van der Waals Heterostructure", Nano Lett. **19**, 1074 (2019).
[43] K. Hatsuda, H. Mine, T. Nakamura, J. Li, R. Wu, S. Katsumoto, J. Haruyama, "Evidence for a quantum spin Hall phase in graphene decorated with Bi2Te3 nanoparticles", Sci. Adv. **4**, 6915 (2018).
[44] K. F. Mak, K. L. McGill, J. Park, P. L. McEuen, "The valley Hall effect in MoS2 transistors", Science, 344, 1489 (2014).
[45] J. Lee, K. F. Mak, J. Shen, "Electrical control of the valley Hall effect in bilayer MoS2 transistors", Nat. Nanotechnol. 11, 421 (2016).
[46] Z. Wu, B. T. Zhou, X. Cai, P. Cheung, G. Liu, M. Huang, J. Lin, T. Han, L. An, Y. Wang, S. Xu, G. Long, C. Cheng, K. T. Law, F. Zhang, N. Wang, "Intrinsic valley Hall transport in atomically thin MoS2", Nat. Commun.

10, 611(2019).
[47] See supplemental Material section 1 for detail of sample fabrication, which includes Refs. [48,49].
[48] H. Kim, N. Leconte, B. L. Chittari, K. Watanabe, T. Taniguchi, A. H. MacDonald, J. Hung, S. Jung, “Accurate gap determination in monolayer and bilayer graphene/h-BN Moire superlattice”, Nano Lett. 18, 7732 (2018).
[49] C. R. Dean, L. Wang, P. Maher, C. Forsythe, F. Ghahari, Y. Gao, J. Katoch, M. Ishigami, P. Moon, M. Koshino, T. Taniguchi, K. Watanabe, K. L. Shepard, J. Hone, P. Kim, “Hofstadter’s butterfly and the fractal quantum Hall effect in moire superlattice”, Nature, 497, 598 (2013).
[50] D. A. Abanin, S. V. Morozov, L. A. Ponomarenko, R. V. Gorbachev, A. S. Mayorov, M. I. Katsnelson, K. Watanabe, T. Taniguchi, K. S. Novoselov, L. S. Levitov, A. K. Geim, “Giant nonlocality near the Dirac point in graphene”, Science 332, 328 (2011).
[51] See supplemental Material section 2 for discussion on other possible origins of nonlocal resistance, which include Refs. [52-56].
[52] Kalon Gopinadhan, Young Jun Shin, Rashid Jalil, Thirumalai Venkatesan, Andre K. Geim, Antonio H. Castro Neto, Hyunsoo Yang, “Extremely large magnetoresistance in few-layer graphene/boron-nitride heterostructures”, Nature Commun. 6, 8337 (2015).
[53] Chang-Ran Wang, Wen-Sen Lu, and Wei-Li Lee, “Transverse thermoelectric conductivity of bilayer graphene in the quantum Hall regime”, Phys. Rev. B 82, 121406 (2010).
[54] R. Ma, L. Zhu, L. Sheng, M. Liu, D. N. Sheng, “Thermoelectric and thermal transport in bilayer graphene”, Phys Rev. B 84, 075420 (2011).
[55] Y. M. Zuev, W. Chang, P. Kim, “Thermoelectric and magnetothermoelectric transport measurements of graphene”, Phys. Rev. Lett. 102, 096807 (2009).
[56] J. G. Checkelsky, G. Checkelsky, N. P. Ong, “Thermopower and Nernst effect in graphene in a magnetic field”, Phys. Rev. B 80, 081413(R) (2009).
[57] See supplemental Material section 4 for relationship between R_L and R_{NL} at finite carrier density.
[58] See supplemental Material section 3 for dual gate dependence in Hall bar 1.
[59] See supplemental Material section 6 for estimation of energy gap of the CAF state.
[60] See supplemental Material section 7 for the measurement of nonlocal resistance due to valley Hall effect in the LP state.
[61] J. Renard, M. Studer, J. A. Folk, “Origins of nonlocality near the neutrality point in graphene”, Phys. Rev. Lett. 112, 116601 (2014).

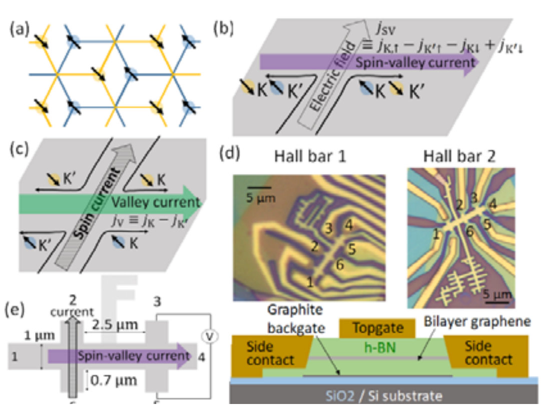

Fig. 1. Spin-valley Hall effect in the CAF state and device structure.
(a) Spin and sublattice configuration of the CAF state in bilayer graphene. Blue (yellow) hexagons are the lattices of the top (bottom) layer. Spins shown as arrows tend to align in each layer but

become opposite between the layers. (b) Schematic description of the spin-valley Hall effect and definition of the spin-valley current. Blue (yellow) circles indicate electrons on the top (bottom) layer, and arrows indicate spin. Spin-valley current is defined as , , where is the current of carriers belonging to the valley K and spin up. (c) Schematic description of the spin current to valley current conversion. The spin current (opposite charge current between the layers) generates the valley current in its transverse direction. (d) Optical microscope images of the two devices used for the experiments (upper panels). The two Hall bars have the same dimension as shown in Fig. 1e. One side of the Hall bar 1 has a jagged region sticking out of the Hall bar between the terminals 2 and 3 to examine the contribution of edge transport to the nonlocal resistance. The lower panel shows the schematic cross section of the device. The bilayer graphene is encapsulated by hexagonal boron nitride with thickness of 35~45 nm, and sandwiched between the top gate and graphite back gate. Hall bar 2 doesn't have graphite back gate and p-doped Si substrate is used as a back gate. (e) Schematic description of the nonlocal transport experiment. A charge current is injected between the terminals 2 and 6, and the nonlocal transport mediated by the spin-valley current is measured as the voltage induced between the terminals 3 and 5.

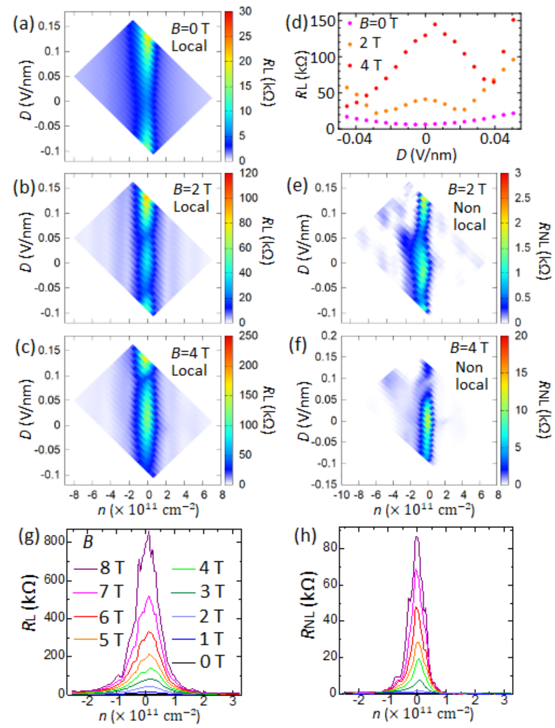

Fig. 2. Carrier density n and displacement field D dependence of the local resistance and nonlocal resistance measured at for Hall bar 2.
(a), (b), (c) n and D dependence of measured at the magnetic field of 0 T (a), 2 T (b), and 4 T (c), respectively. n and D are calculated from the top gate and back gate voltages using the literature value of dielectric constants of h-BN and SiO_2 and measured thickness of h-BN (see supplementary information 3). (d) along the n=0 lines in (a), (b), and (c), showing D dependence for the magnetic fields of 0, 2, and 4 T. (e), (f) n and D dependence of for T (e), and 4 T (f), respectively. (g), (h) n dependence of (g) and (h) along the line, measured at the magnetic field of 0 to 8 T.

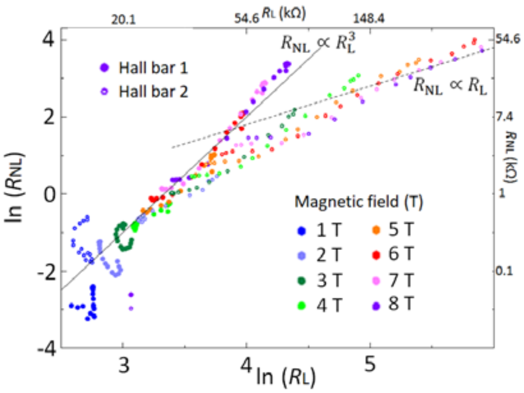

Fig. 3. Scaling relationship between and .

Peak values of along the line plotted as a function of that of obtained in the range of temperature of 1.7 to 32 K and magnetic field of 1 to 8 T. The data points of the same color are taken at the same magnetic field. Dots and open circles denote the data from Hall bar 1 and Hall bar 2, respectively.

The solid (broken) line corresponds to the cubic (linear) scaling.

2817+530+(116+198+120)